frontiers in Energy Research

ORIGINAL RESEARCH
published: 27 July 2021
doi: 10.3389/fenrg.2021.707718

Optimal Locating and Sizing of BESSs in Distribution Network Based on Multi-Objective Memetic Salp Swarm Algorithm

Sui Peng[1], Xianfu Gong[1], Xinmiao Liu[2], Xun Lu[2] and Xiaomeng Ai[3]*

[1]Grid Planning and Research Center, Guangdong Power Grid Corporation, China Southern Power Grid Company Limited, Guangzhou, China, [2]Guangdong Power Grid Corporation, China Southern Power Grid Company Limited, Guangzhou, China, [3]State Key Laboratory of Advanced Electromagnetic Engineering and Technology, School of Electrical and Electronic Engineering, Huazhong University of Science and Technology, Wuhan, China

Battery energy storage systems (BESSs) are a key technology to accommodate the uncertainties of RESs and load demand. However, BESSs at an improper location and size may result in no-reasonable investment costs and even unsafe system operation. To realize the economic and reliable operation of BESSs in the distribution network (DN), this paper establishes a multi-objective optimization model for the optimal locating and sizing of BESSs, which aims at minimizing the total investment cost of BESSs, the power loss cost of DN and the power fluctuation of the grid connection point. Firstly, a multi-objective memetic salp swarm algorithm (MMSSA) was designed to derive a set of uniformly distributed non-dominated Pareto solutions of the BESSs allocation scheme, and accumulate them in a retention called a repository. Next, the best compromised Pareto solution was objectively selected from the repository via the ideal-point decision method (IPDM), where the best trade-off among different objectives was achieved. Finally, the effectiveness of the proposed algorithm was verified based on the extended IEEE 33-bus test system. Simulation results demonstrate that the proposed method not only effectively improves the economy of BESSs investment but also significantly reduces power loss and power fluctuation.

Keywords: distribution networks, battery energy storage systems, optimal locating and sizing, multi-objective memetic salp swarm algorithm, ideal-point decision method

OPEN ACCESS

Edited by:
Bo Yang,
Kunming University of Science and Technology, China

Reviewed by:
Yixuan Chen,
The University of Hong Kong, Hong Kong, SAR China
Yang Li,
Northeast Electric Power University, China

****Correspondence:***
Xinmiao Liu
lxm2021@foxmail.com

Specialty section:
This article was submitted to Smart Grids, a section of the journal Frontiers in Energy Research

Received: *10 May 2021*
Accepted: *07 June 2021*
Published: *27 July 2021*

Citation:
Peng S, Gong X, Liu X, Lu X and Ai X (2021) Optimal Locating and Sizing of BESSs in Distribution Network Based on Multi-Objective Memetic Salp Swarm Algorithm. Front. Energy Res. 9:707718. doi: 10.3389/fenrg.2021.707718

INTRODUCTION

In recent years, distributed generators (DGs) and controllable load in the distribution network (DN) have continued to increase, meaning that the traditional DN faces many challenges (Sepulveda Rangel et al., 2018; Liu et al., 2020; Peng et al., 2020). At present, one obvious tendency is that the rapid-developed photovoltaic (PV) and wind turbine (WT) power generation technologies make the permeability of distributed PV and WT in the DN higher. A series of problems ensue, such as voltage quality declination and power supply reliability reduction, etc (Wang et al., 2014; Yu et al., 2016; Sun et al., 2020). The active power through the line increases at the peak of power load, the loss increases, and a large voltage offset appears at the end of the line (Kerdphol et al., 2016a; Zhou et al., 2021).

Battery energy storage systems (BESSs) have the characteristics of flexibility and fast response and are an effective way to solve the above problems. The application of BESSs can greatly improve the

connection of renewable energy sources (RESs) (Kerdphol et al., 2016b; Gan et al., 2019; Hlal et al., 2019). BESSs can effectively solve the problems of enlarging the load peak and off-peak difference, delay in the power grid upgrading, alleviate the power supply capacity shortage in the transition phase of the power grid, improve the reliability and stability of the power grid, and optimize the power flow of the grid, as well as improving the economic benefits of system operation (Chong et al., 2016; Chong et al., 2018; Murty and Kumar., 2020). BESSs could provide a new direction for large-scale RESs integration, which is one of the most effective ways to solve renewable energy grid access (Trovão and Antunes, 2015; Liu et al., 2018; Wu et al., 2019).

However, prudent BESSs allocation and sizing in DN determine the satisfactory performance of BESSs applications. The optimal allocation and sizing of BESSs are crucial for the power quality improvement of DN and transmission system protection settings. Once BESSs are connected to the DN, the dispatching system of DN sends dispatching instructions to the BESSs according to the real-time running state of the system load, and then BESSs absorbs or sends power to the parallel network through its two-way energy flow (He et al., 2017; Jia et al., 2017; He et al., 2020). This two-way power regulation can save investment and improve the reliability and economy of BESSs. If the location and sizing of BESSs are not set reasonably, or the operation strategy adopted fails to efficiently play the role of BESSs, the voltage quality may deteriorate, and further increase investment and operation costs (Li et al., 2020). To enable us to take full advantage of distributed BESSs and make their access to the DN have a positive impact, it is important to select the appropriate location and sizing of BESSs based on the appropriate operation strategy (Li et al., 2018).

Recently, a large number of scholars have performed studies in this field (Yang et al., 2020). The literature (Oudalov et al., 2007) tends to optimize the location and power capacity of BESSs by calculating the sensitivity of network loss, and then reduce the power loss of DN. In one study (Pang et al., 2019), a semi-definite relaxation method was proposed to solve the optimal BESSs allocation problem. Another study (Wong et al., 2019) introduces a whale optimization algorithm for the optimal location and sizing of BESSs, while the optimization results do not achieve a significant breakthrough.

This paper devises a multi-objective optimization model considering total investment cost, power loss cost, and power fluctuation for optimal BESSs locating and sizing. For the sake of solving this model, a multi-objective memetic salp swarm algorithm (MMSSA) is proposed to search the non-dominated solutions of BESSs allocation strategy, which reach significant improvement and better balance on the global exploration and local exploitation abilities compared with the salp swarm algorithm (SSA). Furthermore, the ideal-point decision method (IPDM) is adapted to objectively determine the optimal weight coefficients of each objective function and then select the best compromised solution. To verify the effectiveness, the proposed model and algorithm are implemented in the extended IEEE-33 bus test system.

The rest of this paper is organized as follows: *Problem Formulation* develops the multi-objective optimization model. In *Multi-Objective Memetic Salp Swarm Algorithm Based on Pareto*, MMSSA based on IPDM is introduced. Case studies are undertaken in *Case Studies*. Finally, *Conclusion* summarizes the main contributions of this study.

TABLE 1 | The economic parameters of BESSs.

Parameters	Values
Installation cost	1470000 ($/per BESS)
Equipment cost	175,000 ($/MW)
	225,000 ($/MW h)
O&M cost	4,000 ($/MW year)
	2000 ($/(MW h) year)
Lifetime	20 (year)

PROBLEM FORMULATION

Objective Functions

The optimal allocation of BESSs is a multi-objective optimization problem with multiple variables and constraints. To realize the economic and reliable operation of BESSs in the DN, a multi-objective optimization model is established based on the Pareto principle, where minimizing the total investment cost of BESSs, power loss cost, and power fluctuation are the main objectives.

Total Investment Cost

This paper focuses on the DN that has been built and operated, so the investment and construction costs of DN other than BESSs are not included in the cost model. The economic parameters of BESSs are provided in **Table 1**, extracted from a previous study (Behnam and Sanna, 2015). The total investment cost is considered as the annual costs of BESSs, which can be mathematically formulated as follows

$$\mathrm{Min}\, F_1 = C_{ins} + C_{equ} + C_{om} \tag{1}$$

where F_1 is the annual total investment cost of BESSs; C_{ins}, C_{equ}, and C_{om} represent the annual installation cost, equipment cost, and operation and maintenance (O&M) cost, respectively.

The annual installation cost of BESSs is expressed as

$$C_{ins} = C_{\mathrm{cap}} \cdot N_{BESS} \cdot \mu_{CRF} \tag{2}$$

where C_{cap} means the cost of per BESS for installation; N_{BESS} is the number of BESSs deployed in DN; μ_{CRF} denotes the capital recovery factor (CRF) that is the knowing present worth. The CRF translates the costs throughout the useful life of BESSs to the initial moment of the investment, which is obtained by

$$\mu_{CRF} = \frac{r \cdot (1+r)^y}{(1+r)^y - 1} \tag{3}$$

where y is the economic life cycle of BESSs; r means the discount rate, which is calculated by the weighted average cost of capital as follows (Harvey, 2020)

$$r = f_{\mathrm{d}} \cdot i_{\mathrm{d}} + \left(1 - f_{\mathrm{d}}\right) \cdot i_{\mathrm{e}} \tag{4}$$

where f_d *and* i_e represent the debt ratio and the return on equity, is respectively, 80 and 50%; i_d denotes the interest rate of 4.165%.

The annual equipment cost of BESSs is calculated by

$$C_{equ} = \sum_{i=1}^{N_{BESS}} \left(\alpha \cdot P_{BESS,i} + \beta \cdot E_{BESS,i}\right) \cdot \mu_{CRF} \tag{5}$$

where α and β mean the costs per unit power and per unit capacity, respectively; $P_{BESS,i}$ and $E_{BESS,i}$ are the power capacity and energy capacity of the ith BESS.

The annual O&M cost of BESSs is expressed as

$$C_{OM} = \sum_{i=1}^{N_{BESS}} \left(\lambda \cdot P_{BESS,i} + \gamma \cdot E_{BESS,i}\right) \cdot \mu_{CRF} \tag{6}$$

where λ and γ are respectively the O&M cost of per unit power and per unit energy of BESSs. Note that the O&M costs of rectifier, inverter, and charge regulator are neglected.

Power Loss Cost

BESSs grid-connected will change the power flow of DN (Injeti and Thunuguntla, 2020). Furthermore, the different locations and sizes of BESSs will have different influences on power losses. For the sake of minimizing the total active power losses, the power losses index is established in the optimization model, as follows

$$\text{Min } F_2 = \sum_{t=1}^{T} \left(\rho_{loss}(t) \cdot P_{loss}(t)\right) \tag{7}$$

$$P_{loss}(t) = \sum_{j=1}^{L} \left(R_j I_j^2(t)\right) \tag{8}$$

where F_2 is the daily cost of power losses; $\rho_{loss}(t)$ and $P_{loss}(t)$ represent the time of use (TOU) electricity prices and power losses at time t; L is the total number of lines in the DN; R_j means the resistance on the jth line; $I_j(t)$ denotes the current on the jth line at time t. The lower F_2 is that the greater positive effect of BESSs deployment in reducing power loss.

Power Fluctuation

Owing to the intermittent nature of RESs, the integration of them into power grids poses significant power fluctuation in the grid connection point. However, BESSs can provide an effective supplement for RESs in smoothing power fluctuation to improve power quality. The power quality index can be expressed as

$$\text{Min } F_3 = \sqrt{\sum_{t=1}^{T} \left(P_{grid}(t) - \overline{P}_{grid}\right)^2} \tag{9}$$

where F_3 is the daily total power fluctuation of the grid connection point; $P_{grid}(t)$ represents the power fluctuation at time t; $\overline{P}_{grid}$ means the mean power fluctuation over a day.

Constraints

Power Balance

$$\begin{cases} P_i(t) = V_i(t) \sum_{j=1}^{N} V_j(t)\left(G_{ij}\cos\theta_{ij}(t) + B_{ij}\sin\theta_{ij}(t)\right) \\ Q_i(t) = V_i(t) \sum_{j=1}^{N} V_j(t)\left(G_{ij}\sin\theta_{ij}(t) - B_{ij}\cos\theta_{ij}(t)\right) \end{cases} \tag{10}$$

where $P_i(t)$ and $Q_i(t)$ represent the injected active power and reactive power at ith node in the DN at time t, respectively; $V_i(t)$ is the voltage of the ith node at time t; G_{ij} and B_{ij} represent the admittance and susceptance between the ith node and the jth node; $\theta_{ij}(t)$ is the power angle between the ith node and the jth node at time t.

Range of Node Voltages

$$V_i^{\min} < V_i < V_i^{\max} \tag{11}$$

where $V_i^{\min}$ and $V_i^{\max}$ represent the upper and lower limits of the voltages of the ith node.

Charging and Discharging Power Limits of BESSs

$$\begin{cases} 0 \le P_{cha,i}(t) \le P_{BESS,i} \cdot \eta_{cha} \\ -P_{BESS,i} \cdot \eta_{dis} \le P_{dis,i}(t) \le 0 \end{cases} \tag{12}$$

where $P_{cha,i}(t)$ and$P_{dis,i}(t)$ represent the charging and discharging power of BESSs at time t, respectively; η_{cha} and η_{dis} are respectively the charging and discharging efficiency of BESSs.

State of Charge Limits

$$SOC^{\min} < SOC(t) < SOC^{\max} \tag{13}$$

where $SOC^{\min}$ and $SOC^{\max}$, respectively, mean the upper and lower limits of SOC, is that 20 and 90%.

Multi-Objective Optimization Model

Establishment of the Optimization Model

In terms of multi-objective optimization problems such as BESSs allocation, all objectives generally conflict with each other, and optimizing one of the objectives leads to the deterioration of other objectives in most cases. It is difficult to objectively evaluate the superiority-inferiority of all solutions because there is no absolute optimal solution for the overall objective (Huang et al., 2020). Nevertheless, there exists an optimal solution set, elements of which are named Pareto optimal solutions, realizing the optimum matching among objectives (Fonseca and Fleming, 1993). In this paper, the multi-objective optimization model of BESSs locating and sizing is designed to simultaneously meet investment economy and operation reliability requirements, as follows

$$\begin{cases} \min \boldsymbol{F}(x) = [F_1(\boldsymbol{x}), F_2(\boldsymbol{x}), F_3(\boldsymbol{x})]^{\mathrm{T}} \\ \text{s.t.} E(\boldsymbol{x}) = 0 \\ I(\boldsymbol{x}) \le 0 \end{cases} \tag{14}$$

where $\boldsymbol{F}(\boldsymbol{x})$ represents the target space consists of all objective functions; $\boldsymbol{x}$ denotes the decision space that is constituted by all optimization variables; $E(\boldsymbol{x})$ and $I(\boldsymbol{x})$ are respectively, equality and inequality constraints that need to be satisfied in the multi-objective optimization model.

Design of Optimization Variables

Optimization variables include the installation locations, power, and energy capacities of two BESSs, all of which need to be constructed in a reasonable range, otherwise, some negative effects on the power flow, relay protection, voltage, and waveform of the original power grid raise. In this paper, nodes in the range of (Mirjalili et al., 2017; Liu et al., 2020) were selected as the installation locations, in which environmental and geographical factors need to be considered in engineering practice. The limits of power and energy capacities are determined to consider the topology of DN, the power limit of the interconnection point, especially the total load power. Therefore, the power capacity allowed to access the power grid of a BESS is determined as 90% of the total active power load of the power grid, and the numerical value of energy capacity limit is equal to power capacity limit, as follows

$$\begin{cases} P_{BESS,i} \le P_{BESS}^{\max} \\ E_{BESS,i} \le E_{BESS}^{\max} \end{cases} \tag{15}$$

where $P_{BESS,i}$ and $E_{BESS,i}$ are the power capacity and energy capacity of the ith BESS; $P_{BESS}^{\max}$ and $E_{BESS}^{\max}$ denote the upper limits of the energy capacity and power capacity of BESSs, are respectively, 3375 and 3375 kWh.

Note that the power and energy capacities of two BESSs are continuous, while installation locations are discrete. In this paper, continuous variables can converge to the optimal value in the iteration process while the optimal value of discrete variables needs to be rounded in continuous space (Zhang et al., 2017).

MULTI-OBJECTIVE MEMETIC SALP SWARM ALGORITHM BASED ON PARETO

Memetic Salp Swarm Algorithm

Optimization Framework

SSA is inspired by the swarming motility and foraging behavior of salps, which successfully solves varieties of optimization problems since it has a simple search mechanism and high optimization efficiency (Mirjalili et al., 2017). In recent years, the memetic algorithm has developed into a broad class of algorithms and can properly combine global search and local search mechanisms (Moscato, 1989; Neri and Cotta, 2012). In this paper, the memetic computing framework first proposed by Moscato (Moscato, 1989) is adopted in the memetic salp swarm algorithm (MSSA) to improve the searching ability of SSA. Then, multiple slap chains were employed to better balance global exploration and local exploitation abilities. Therefore, there are two important search mechanisms in MSSA, namely the local search in a single chain and the global coordination in the whole population. In MSSA, multiple salp chains are arranged in parallel, where each salp chain is regarded as a swarm of salps that independently perform local searches similar to SSA. Meanwhile, all salp chains are regrouped by information communication among all salps for the improvement of convergence stability. The optimization framework of MSSA is illustrated in **Figure 1**.

Mathematical Model

In the single chain, the salps can be divided into two roles, including the leaders and the followers. As illustrated in **Figure 1**, the leader is regarded as the salp at the front of each salp chain, while the rest of the salps are followers. In each iteration, the leading salp seeks the food source, while the follower salps follow each other in a row. Note that the best salp with the best fitness is considered to be the food source, and will be chased by the whole salp chain. The position of the leading salp and follower salps can be updated as follows (Mirjalili et al., 2017)

$$x_{m1}^{j} = \begin{cases} F_m^j + c_1\left(c_2\left(ub^j - lb^j\right) + lb^j\right), & if\ c_3 \ge 0 \\ F_m^j - c_1\left(c_2\left(ub^j - lb^j\right) + lb^j\right), & if\ c_3 < 0 \end{cases} \tag{16}$$

$$x_{mi}^{j} = \frac{1}{2}\left(x_{mi}^{j} + x_{m,i-1}^{j}\right), \quad i = 2, 3, \ldots, n;\ m = 1, 2, \ldots, M \tag{17}$$

where the j means the jth dimension of searching space; x_{m1}^{j} and x_{mi}^{j} respectively denote the positions of the leading salp and the ith follower salp in the mth salp chain; F_m^j is the position of a food source; ub^j and lb^j are respectively the upper and lower limits of the jth dimension variables; n and M represent the population size of a single salp chain and the number of salp chains, respectively; c_2, and c_3 are both the uniform random numbers from 0 to 1; c_1 is a random number that is related to the iteration number, as follows (Mirjalili et al., 2017)

$$c_1 = 2\mathrm{e}^{-\left(\frac{4k}{k_{\max}}\right)^2} \tag{18}$$

where k and $k_{\max}$ are the current iteration number and maximum iteration number, respectively.

In the salp population, each salp is taken as an individual of the virtual salp population. At each iteration, the population can be regrouped into multiple new salp chains based on the descending order of all salps' fitness values. In the regroup operation, the global coordination among different salp swarms is achieved, as shown in **Figure 2**. It can be seen that the best solution is assigned to salp chain #1, and then the second-best solution is assigned to salp chain #2, and so on. Therefore, the mth salp chain can be updated by (Eusuff and Lansey, 2015)

$$\begin{gathered} \boldsymbol{Y}^m = \left[\boldsymbol{x}_{mi}, f_{mi} | \boldsymbol{x}_{mi} = \boldsymbol{X}(m + M(i-1)),\right. \\ \left. f_{mi} = \boldsymbol{F}(m + M(i-1)),\ i = 1, 2, \cdots, n\right],\ \ m = 1, 2, \cdots, M \end{gathered} \tag{19}$$

where $\boldsymbol{x}_{mi}$ and f_{mi} are the position vector and fitness value of the ith salp in the mth chain, respectively; $\boldsymbol{X}$ and $\boldsymbol{F}$ denote a position vector set and a fitness value set of all the salps, respectively.

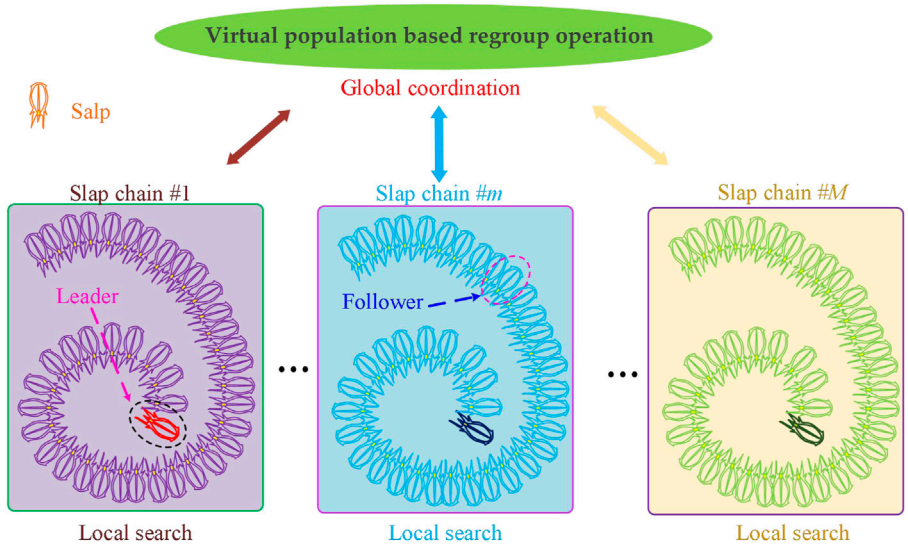

FIGURE 1 | Conceptual optimization framework of MSSA.

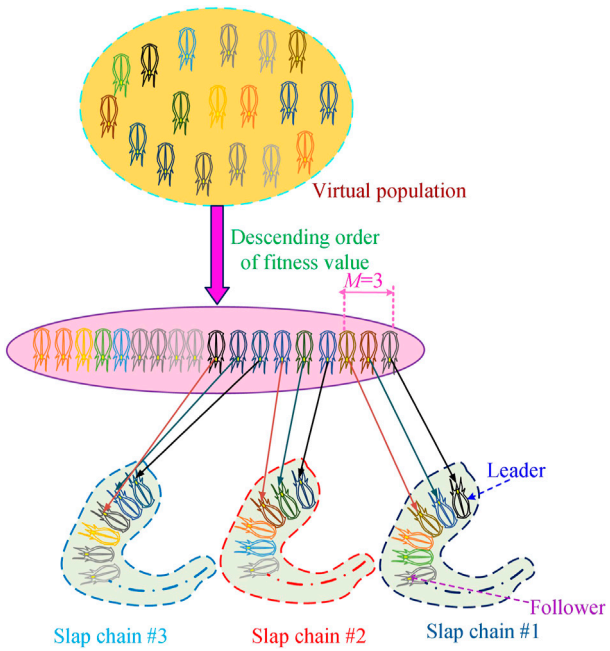

FIGURE 2 | Regroup operation of salp population for global coordination.

Multi-Objective Memetic Salp Swarm Algorithm

As discussed in *Problem Formulation*, the solutions for a multi-objective problem should be a set of Pareto optimal solutions. MSSA can drive salps towards the food source with the best solution for the optimization problem and update it at each iteration. The design of MMSSA is first to equip the food sources with a repository to restore the non-dominated solutions obtained by MSSA so far (Coello et al., 2004). In the optimization process, every new non-dominated solution needs to be compared against all residents in the repository using the Pareto dominance operators, as follows (Faramarzi et al., 2020).

- If a new solution dominates a set of solutions in the repository, they have to be swapped;
- If at least one of the solutions in the repository dominates the new solution, this new solution should be discarded straight away;
- If a new solution is non-dominated in comparison with all repository residents, this new solution will be added to the repository.

The repository can just store limited solutions. Therefore, a wise method adopted to remove the similar non-dominated solutions in the repository, is that the one in the populated region is identified as the best candidate to be removed from the repository to improve the distribution diversity of the Pareto optimal solution set. The solutions that are removed from the repository need to satisfy the following equation

$$\begin{cases} |F_h(x_m) - F_h(x_n) < D_h|,\ h = 1,\ 2,\ 3 \\ D_h = \dfrac{F_h^{\max} - F_h^{\min}}{N_r} \end{cases} \tag{20}$$

where $F_h(x_m)$ and $F_h(x_n)$ denote the hth fitness value of the mth salp and the nth salp, respectively; D_h is the distance threshold of the Pareto solution set; $F_h^{\max}$ and $F_h^{\min}$, respectively, represent the maximum and minimum of the hth objective function obtained as far; N_r is the maximum size of the repository to store the non-dominated solutions.

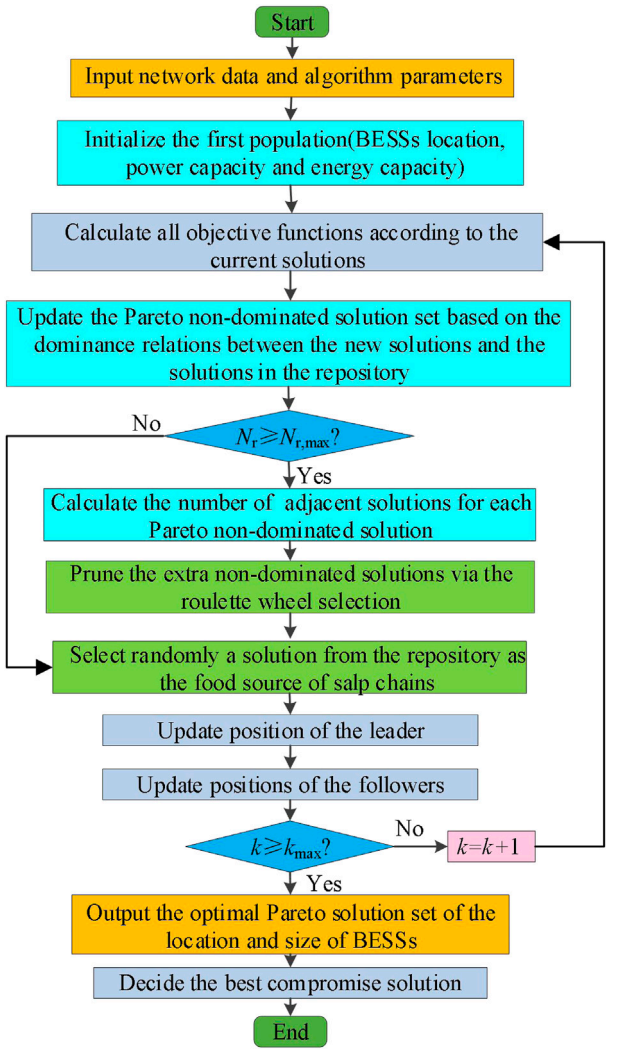

FIGURE 3 | The flowchart of MMSSA for the optimal locating and sizing of BESSs.

In this paper, the IPDM was adopted to filter out the best compromised solution of the Pareto non-dominated solution set, which is often used in multiple attribute decision making. Firstly, the objective functions of all Pareto non-dominated solutions obtained by MPOA are normalized as follows

$$f_h(x_m) = \frac{y_h(x_m) - y_h^{\min}}{y_h^{\max} - y_h^{\min}} \tag{21}$$

where $y_h(x_m)$ is the hth objective function value of the non-dominated solution x_m; $f_h(x_m)$ represents the normalized value of the hth objective function; $y_h^{\min}$ and $y_h^{\max}$ mean the maximum and minimum of the hth objective function.

Thus, an ideal point can be selected in the target decision-making region formed by all Pareto non-dominated solutions. It is worth mentioning that the objective functions of the ideal point can be normalized to be (0, 0, 0) in terms of the minimization problem. Crucially, the squared Euclidean distance between different solutions and the ideal point is taken as an important basis for ranking all non-dominated solutions and then decide the best compromised solution from them. The squared Euclidean distance can be calculated by

$$EU_i = \sum_{h=1}^{3} \left[f_h(x_m) - 0 \right]^2 \cdot \omega_h^2 \tag{22}$$

ω_h means the weights of the hth objective function, as follows

$$\omega_h = \frac{1}{\sum_{m=1}^{N_r} \left[f_h(x_m) - 0 \right]^2 \cdot \sum_{h=1}^{3} \frac{1}{\sum_{m=1}^{N_r} \left[f_h(x_m) - 0 \right]^2}} \tag{23}$$

Owing to the weights of each objective function obtained by IPDM, it does not rely on the evaluation and preference of experts so that the decision is credible. In the end, the best compromised solution is expressed as

$$x_{best} = \arg \min_{m=1,2,\ldots,N_r} \sum_{h=1}^{3} \left[f_h(x_m) - 0 \right]^2 \cdot \omega_h^2 \tag{24}$$

To sum up, the flowchart of MMSSA to solve the optimal locating and sizing of BESSs is shown in **Figure 3**.

CASE STUDIES

Test System

In this section, the optimal locating and sizing of BESSs based on MMSSA is implemented in the extended IEEE-33 bus system for verifying the effectiveness of the proposed algorithm. The topology structure of the test system with a total load of 3,715 + *j*2300 kVA is depicted in **Figure 4**. It is assumed that the resource units include one PV and three WT, where the maximum generation limits of PV and WT both are 0.2 MW. The typical daily curves of load, wind and PV power are demonstrated in **Figure 5**. In addition, multi-objective particle swarm optimization (MOPSO) (Hlal et al., 2019) is used for

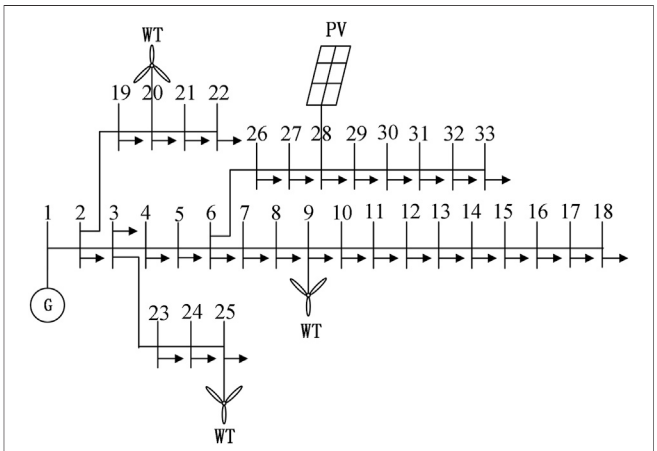

FIGURE 4 | Extended IEEE-33 bus test system.

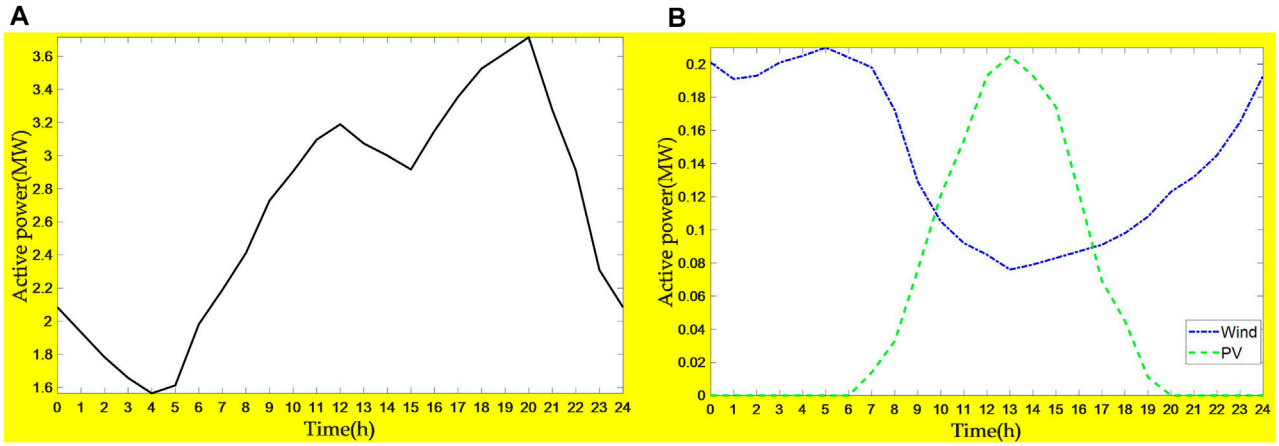

FIGURE 5 | Typical daily curves: **(A)** hourly load curves; **(B)** hourly wind and PV power curves.

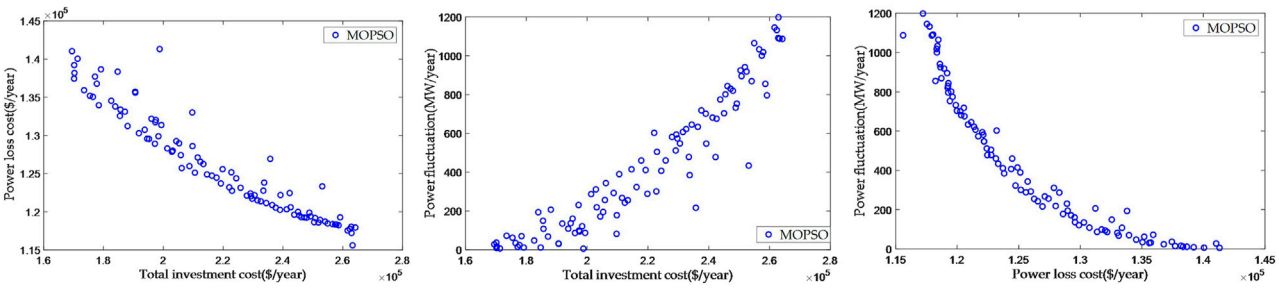

FIGURE 6 | Three-objective Pareto front results obtained by MOPSO.

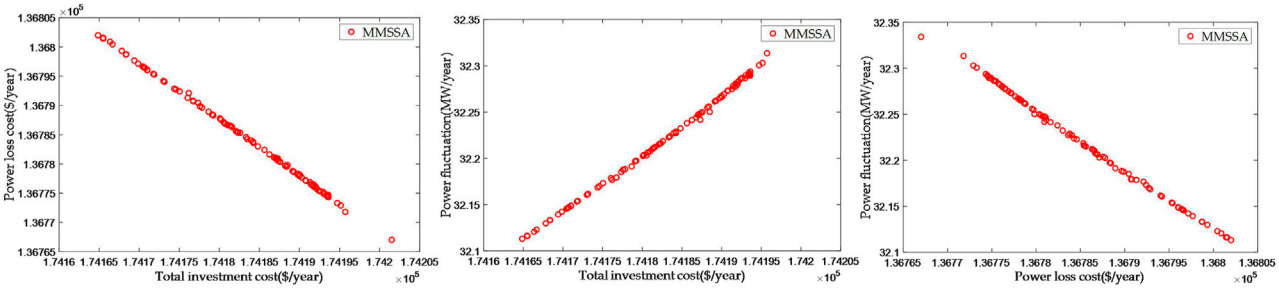

FIGURE 7 | Bi-objective Pareto front results obtained by MMSSA.

comparison. For the sake of a relatively fair comparison, the population size of MMSSA and other algorithms all are set to 100, and the maximum iterations are set to be 500. The size of the repository was chosen to equal 100 for multi-objective optimization. Some specific parameters of all comparison algorithms were set to the default values. If the parameters are not chosen properly, the convergence time will be too long or the local optimum will be trapped. It is worth mentioning that the key parameters in the MMSSA algorithm, such as $c1$, the most important parameter since they can directly influence the trade-off between exploration and exploitation. To achieve a proper balance, it was designed according to the iteration number.

Simulation Results

Figure 6 and **Figure 7**, respectively, exhibit the bi-objective Pareto front curves by two algorithms, including the total investment cost versus the power loss cost, the total investment cost versus the power fluctuation, as well as the power loss cost versus power fluctuation, which demonstrates these three bi-objective Pareto fronts obtained by MMSSA are

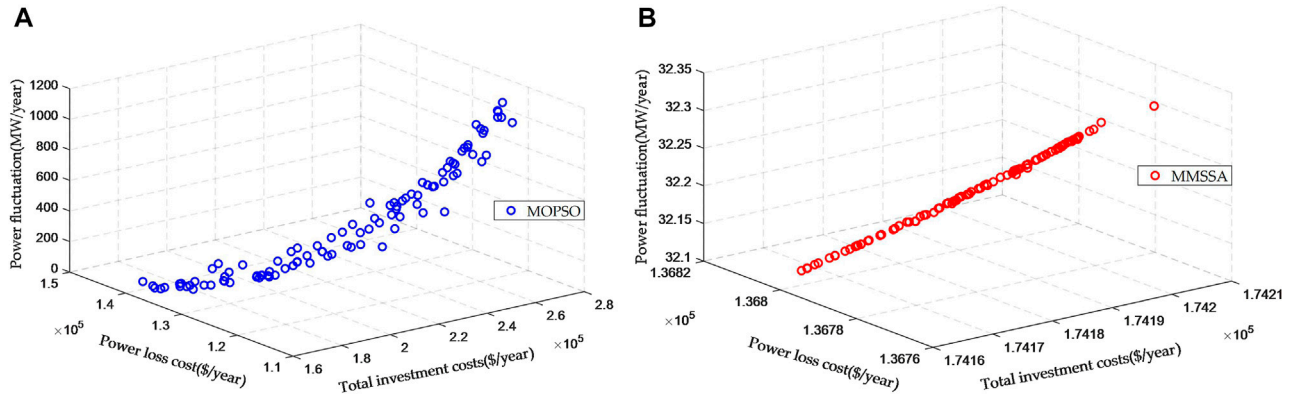

FIGURE 8 | Three-objective Pareto front results obtained by two algorithms: **(A)** MOPSO; **(B)** MMSSA.

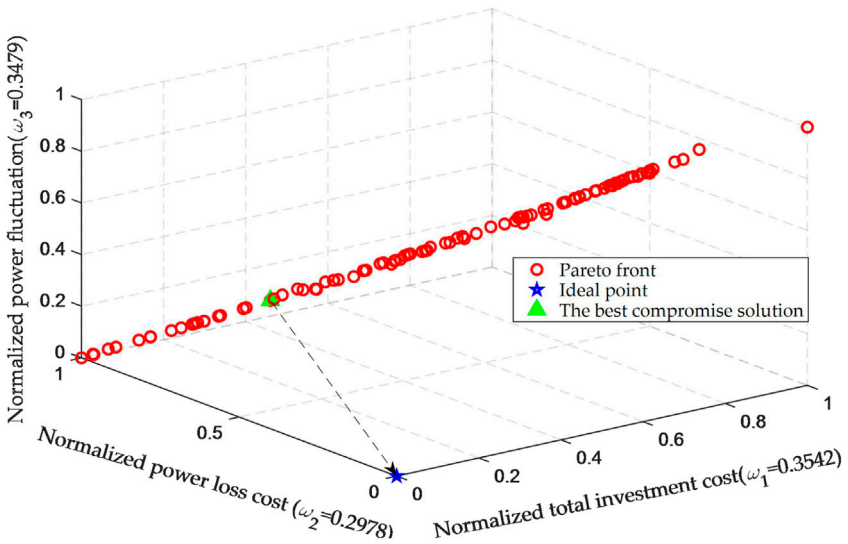

FIGURE 9 | The schematic diagram of IPDM based on MMSSA.

more uniform than MOPSO from the perspective of distribution. **Figure 8** shows the three-objective Pareto front obtained by two algorithms. As can be seen from **Figure 8**, MMSSA can acquire the Pareto solution set with higher quality compared with MOPSO. Moreover, the schematic diagram of the IPDM based on MMSSA is illustrated in **Figure 9**. **Figure 9** shows the normalized objective function curve based on MMSSA, as well as the decision-making schematic for the best compromise solution of BESSs allocation. IPDM based on MMSSA can obtain the objective weight coefficients and select the best compromise solution by means of the sum of squares of Euclidean distance.

To better compare the convergence and diversity of the Pareto solution set obtained by two algorithms, the performance indexes are evaluated in **Table 2**, including coverage over the Pareto front (CPF) (Tian et al., 2019), spread (Wang et al., 2010), spacing (Schott, 1995), and execution time. It is worth mentioning that CPF defines the diversity of Pareto solution set as its coverage over the Pareto front in an (*M*-1) dimensional hypercube (Wang et al., 2010), while spread and spacing respectively denote the diversity and the evenness of the Pareto solution set, which are all the negative indexes. In addition, **Table 3** shows the best compromise decision scheme of BESSs allocation from two algorithms, along with the objective function values. It is evident that the MMSSA outperforms the MOPSO in the multi-objective optimization model for optimal locating and sizing of BESSs:

TABLE 2 | Comparison of performance metrics of two algorithms.

Algorithm	Performance metric			
	CPF	Spread	Spacing	Time (s)
MOPSO	0.4996	0.4753	9,075.45	1.5428e+04
MMSSA	0.1636	0.4481	3.3858	1.4676e+04

TABLE 3 | Optimization results of two algorithms.

Algorithm	The best compromise allocation scheme of BESSs			Objective function values under the best compromise allocation scheme		
	Bus location	Power capacity (MW)	Energy capacity (MW·h)	Total investment cost ($/year)	Power loss cost ($/year)	Power fluctuation (MW/year)
MOPSO	Trovão and Antunes (2015); Mirjalili et al. (2017)	[0.1972, 0.2786]	[1.6203, 1.6204]	2.0873e+05	1.3698e+05	292.9054
MMSSA	Pang et al. (2019); Injeti and Thunuguntla (2020)	[0.0849, 0.0618]	[0.6535, 0.3943]	1.7417e+05	1.3679e+05	32.1682

- It has the smallest CPF value, indicating that MMSSA owns better diversity;
- It gains the smallest spread and spacing value, which indicates that the Pareto solutions obtained by MMSSA are evenly and widely distributed on the Pareto front;
- It also has the smallest execution time, which means that MMSSA can converge to the Pareto front much faster than conventional MOPSO;
- It has the least investment cost, meaning that MMSSA can improve the economy of BESSs investment;
- It slightly reduces power loss cost, and ensures a higher operation economy of DN;
- It significantly gains lower power fluctuation of the grid connection point, which means MMSSA can contribute to power supply reliability.

CONCLUSION

In this paper, a multi-objective optimization model based on the Pareto principle was established. This study proposes MMSSA as a method for solving the optimal location and size of BESSs in DN. The contributions of the proposed approach are as follows:

- The multi-objective optimization model takes the economic criteria, incorporates time value into cost, and the technical criteria relate to system reliability and take it into consideration, which aims to make BESSs more cost-effective and ensure the reliable operation of DN;
- The proposed MMSSA has a strong global search ability and convergence ability under complex multi-objective functions, which can quickly search high-quality non-dominated solutions, and then objectively select the best compromised solution with the help of IPDM;
- The simulation results based on the extended IEEE-33 bus test system effectively verify that the best-compromised solution of BESSs allocation scheme obtained by MMSSA owns the lowest investment cost, power loss cost, and power fluctuation, which is beneficial for DN to increase economic efficiency and improve system reliability.

However, there are several limitations to this work, including the inapplicability of the proposed MMSSA for the high-dimension optimization problem, and the limited scenario design in terms of validating its effectiveness. Therefore, the MMSSA can be further enhanced to improve the accuracy for high-dimensional objective optimization. Meanwhile, a multi-scenario design that combines different typical daily data in a year should be conducted to capture the time-variable nature and uncertainties related to RESs and load demand.

DATA AVAILABILITY STATEMENT

The original contributions presented in the study are included in the article/supplementary material, further inquiries can be directed to the corresponding author.

AUTHOR CONTRIBUTIONS

SP and XG contributed to conception and design of the study. XiL and XuL performed the case analysis. SP wrote the first draft of the manuscript. XG, XiL, XuL, and XA wrote sections of the article. All authors contributed to article revision, read, and approved the submitted version.

FUNDING

The paper is funded by the project supported by the China Southern Power Grid Science and Technology Project under Project 037700KK52190011 (GDKJXM20198273).

ACKNOWLEDGMENTS

The authors gratefully acknowledge that this project was supported by the China Southern Power Grid Science and Technology Project under Project 037700KK52190011 (GDKJXM20198273).

REFERENCES

Behnam, Z., and Sanna, S. (2015). Electrical Energy Storage Systems: A Comparative Life Cycle Cost Analysis. *Renew. Sust. Energ. Rev.* 42, 569–596. doi:10.1016/j.rser.2014.10.011

Chong, L. W., Wong, Y. W., Rajkumar, R. K., and Isa, D. (2018). An Adaptive Learning Control Strategy for Standalone PV System with Battery-Supercapacitor Hybrid Energy Storage System. *J. Power Sourc.* 394, 35–49. doi:10.1016/j.jpowsour.2018.05.041

Chong, L. W., Wong, Y. W., Rajkumar, R. K., and Isa, D. (2016). An Optimal Control Strategy for Standalone PV System with Battery-Supercapacitor Hybrid

Energy Storage System. *J. Power Sourc.* 331, 553–565. doi:10.1016/j.jpowsour.2016.09.061

Coello, C. A. C., Pulido, G. T., and Lechuga, M. S. (2004). Handling Multiple Objectives with Particle Swarm Optimization. *Evol. Comput. IEEE Trans.* 8, 256–279. doi:10.1109/tevc.2004.826067

Eusuff, M. M., and Lansey, K. E. (2015). Optimization of Water Distribution Network Design Using the Shuffled Frog Leaping Algorithm. *J. Water Resour. Plann. Manag.* 129 (3), 210–225. doi:10.1061/40569(2001)412

Faramarzi, A., Heidarinejad, M., and Stephens, b. (2020). Equilibrium Optimizer: a Novel Optimization Algorithm. *Knowledge Based Syst.* 191, 105190. doi:10.1016/j.knosys.2019.105190

Fonseca, C. M., and Fleming, P. J. (1993). Genetic Algorithms for Multiobjective Optimization: Formulation Discussion and Generalization. *Icga* 93, 416–423.

Gan, W., Ai, X., Fang, J., Yan, M., Yao, W., Zuo, W., et al. (2019). Security Constrained Co-planning of Transmission Expansion and Energy Storage. *Appl. Energ.* 239, 383–394. doi:10.1016/j.apenergy.2019.01.192

Harvey, H. L. D. (2020). Clarifications of and Improvements to the Equations Used to Calculate the Levelized Cost of Electricity (LCOE), and Comments on the Weighted Average Cost of Capital (WACC). *Energy* 207, 118340. doi:10.1016/j.energy.2020.118340

He, X., Ai, Q., Qiu, R. C., Huang, W. T., Piao, L. J., and Liu, H. C. (2017). A Big Data Architecture Design for Smart Grids Based on Random Matrix Theory. *IEEE Trans. Smart Grid.* 8 (2), 674–686.

He, X., Qiu, R. C., Ai, Q., and Zhu, T. Y. (2020). A Hybrid Framework for Topology Identification of Distribution Grid with Renewables Integration. *IEEE Trans. Power Syst.* 36 (2), 1493–1503. doi:10.1109/tpwrs.2020.3024955

Hlal, M. I., Ramachandaramurthya, V. K., Padmanaban, S., Kaboli, H. R., Pouryekta, A., and Tuan Abdullah, T. A. R. b. (2019). NSGA-II and MOPSO Based Optimization for Sizing of Hybrid PV/wind/battery Energy Storage System. *Ijpeds* 10 (1), 463–478. doi:10.11591/ijpeds.v10.i1.pp463-478

Huang, Z., Fang, B. L., and Deng, J. (2020). Multi-objective Optimization Strategy for Distribution Network Considering V2G Enabled Electric Vehicles in Building Integrated Energy System. *Prot. Control. Mod. Power Syst.* 5 (1), 48–55. doi:10.1186/s41601-020-0154-0

Injeti, S. K., and Thunuguntla, V. K. (2020). Optimal Integration of DGs into Radial Distribution Network in the Presence of Plug-In Electric Vehicles to Minimize Daily Active Power Losses and to Improve the Voltage Profile of the System Using Bioinspired Optimization Algorithms. *Prot. Control. Mod. Power Syst.* 5 (1), 21–35. doi:10.1186/s41601-019-0149-x

Jia, K., Chen, Y., Bi, T., Lin, Y., Thomas, D., and Sumner, M. (2017). Historical-data-based Energy Management in a Microgrid with a Hybrid Energy Storage System. *IEEE Trans. Ind. Inf.* 13 (5), 2597–2605. doi:10.1109/tii.2017.2700463

Kerdphol, T., Fuji, K., Mitani, Y., Watanabe, M., and Qudaih, Y. (2016). Optimization of a Battery Energy Storage System Using Particle Swarm Optimization for Stand-Alone Microgrids. *Int. J. Electr. Power Energ. Syst.* 81, 32–39. doi:10.1016/j.ijepes.2016.02.006

Kerdphol, T., Qudaih, Y., and Mitani, Y. (2016). Optimum Battery Energy Storage System Using PSO Considering Dynamic Demand Response for Microgrids. *Int. J. Electr. Power Energ. Syst.* 83, 58–66. doi:10.1016/j.ijepes.2016.03.064

Li, R., Wang, W., Chen, Z., and Wu, X. (2018). Optimal Planning of Energy Storage System in Active Distribution System Based on Fuzzy Multi-Objective Bi-level Optimization. *J. Mod. Power Syst. Clean. Energ.* 6 (2), 342–355. doi:10.1007/s40565-017-0332-x

Li, Y., Vilathgamuwa, M., Choi, S. S., Xiong, B., Tang, J., Su, Y., et al. (2020). Design of Minimum Cost Degradation-Conscious Lithium-Ion Battery Energy Storage System to Achieve Renewable Power Dispatchability. *Appl. Energ.* 260, 114282. doi:10.1016/j.apenergy.2019.114282

Liu, J., Yao, W., Wen, J., Fang, J., Jiang, L., He, H., et al. (2020). Impact of Power Grid Strength and PLL Parameters on Stability of Grid-Connected DFIG Wind Farm. *IEEE Trans. Sustain. Energ.* 11 (1), 545–557. doi:10.1109/tste.2019.2897596

Liu, Z., Chen, Y., Zhuo, R., and Jia, H. (2018). Energy Storage Capacity Optimization for Autonomy Microgrid Considering CHP and EV Scheduling. *Appl. Energ.* 210, 1113–1125. doi:10.1016/j.apenergy.2017.07.002

Mirjalili, S., Gandomi, A. H., Mirjalili, S. Z., Saremi, S., Faris, H., and Mirjalili, S. M. (2017). Salp Swarm Algorithm: A Bio-Inspired Optimizer for Engineering Design Problems. *Adv. Eng. Softw.* 114, 163–191. doi:10.1016/j.advengsoft.2017.07.002

Moscato, P. (1989). On Evolution, Search, Optimization, Genetic Algorithms and Martial Arts: Towards Memetic Algorithms. Caltech Concurrent Computation Program, Technical Reports 826.

Murty, V. V. S. N., and Kumar, A. (2020). Multi-objective Energy Management in Microgrids with Hybrid Energy Sources and Battery Energy Storage Systems. *Prot. Control. Mod. Power Syst.* 5 (1), 1–20. doi:10.1186/s41601-019-0147-z

Neri, F., and Cotta, C. (2012). Memetic Algorithms and Memetic Computing Optimization: A Literature Review. *Swarm Evol. Comput.* 2, 1–14. doi:10.1016/j.swevo.2011.11.003

Oudalov, A., Chartouni, D., and Ohler, C. (2007). Optimizing a Battery Energy Storage System for Primary Frequency Control. *IEEE Trans. Power Syst.* 22 (3), 1259–1266. doi:10.1109/tpwrs.2007.901459

Pang, M., Shi, Y., Wang, W., and Pang, S. (2019). Optimal Sizing and Control of Hybrid Energy Storage System for Wind Power Using Hybrid Parallel PSO-GA Algorithm. *Energy. explorat & exploitat.* 37 (1), 558–578. doi:10.1177/0144598718784036

Peng, X., Yao, W., Yan, C., Wen, J., and Cheng, S. (2020). Two-stage Variable Proportion Coefficient Based Frequency Support of Grid-Connected DFIG-WTs. *IEEE Trans. Power Syst.* 35 (2), 962–974. doi:10.1109/tpwrs.2019.2943520

Schott, J. R. (1995). *Fault Tolerant Design Using Single and Multicriteria Genetic Algorithm Optimization*. Cambridge, MA: Massachusetts Institute of Technology.

Sepulveda Rangel, C. A., Canha, L., Sperandio, M., and Severiano, R. (2018). Methodology for ESS-type Selection and Optimal Energy Management in Distribution System with DG Considering Reverse Flow Limitations and Cost Penalties. *IET Generation, Transm. Distribution.* 12 (5), 1164–1170. doi:10.1049/iet-gtd.2017.1027

Sun, K., Yao, W., Fang, J., Ai, X., Wen, J., and Cheng, S. (2020). Impedance Modeling and Stability Analysis of Grid-Connected DFIG-Based Wind Farm with a VSC-HVDC. *IEEE J. Emerg. Sel. Top. Power Electron.* 8 (2), 1375–1390. doi:10.1109/jestpe.2019.2901747

Tian, Y., Cheng, R., Zhang, X., Li, M., and Jin, Y. (2019). Diversity Assessment of Multi-Objective Evolutionary Algorithms: Performance Metric and Benchmark Problems. *IEEE Comput. Intelligence Mag.* 14 (3), 61–74. doi:10.1109/mci.2019.2919398

Trovão, J. P., and Antunes, C. H. (2015). A Comparative Analysis of Meta-Heuristic Methods for Power Management of a Dual Energy Storage System for Electric Vehicles. *Energ. Convers. Manag.* 95, 281–296. doi:10.1016/j.enconman.2015.02.030

Wang, B., Yang, Z., Lin, F., and Zhao, W. (2014). An Improved Genetic Algorithm for Optimal Stationary Energy Storage System Locating and Sizing. *Energies* 7 (10), 6434–6458. doi:10.3390/en7106434

Wang, Y., Wu, L., and Yuan, X. (2010). Multi-objective Self-Adaptive Differential Evolution with Elitist Archive and Crowding Entropy-Based Diversity Measure. *Soft Comput.* 14 (3), 193–209. doi:10.1007/s00500-008-0394-9

Wong, L. A., Ramachandaramurthy, V. K., Walker, S. L., Taylor, P., and Sanjari, M. J. (2019). Optimal Placement and Sizing of Battery Energy Storage System for Losses Reduction Using Whale Optimization Algorithm. *J. Energ. Storage.* 26, 100892. doi:10.1016/j.est.2019.100892

Wu, T., Shi, X., Liao, L., Zhou, C., Zhou, H., and Su, Y. (2019). A Capacity Configuration Control Strategy to Alleviate Power Fluctuation of Hybrid Energy Storage System Based on Improved Particle Swarm Optimization. *Energies* 12 (4), 642. doi:10.3390/en12040642

Yang, B., Wang, J., Chen, Y., Li, D., Zeng, C., Guo, Z., et al. (2020). Optimal Sizing and Placement of Energy Storage System in Power Grids: a State-Of-The-Art

One-Stop Handbook. *J. Energ. Storage.* 32, 101814. doi:10.1016/j.est.2020.101814

Yu, H., Tarsitano, D., Hu, X., and Cheli, F. (2016). Real Time Energy Management Strategy for a Fast Charging Electric Urban Bus Powered by Hybrid Energy Storage System. *Energy* 112, 322–331. doi:10.1016/j.energy.2016.06.084

Zhang, X. S., Yu, T., Yang, B., and Cheng, L. F. (2017). Accelerating Bio-Inspired Optimizer with Transfer Reinforcement Learning for Reactive Power Optimization. *Knowledge-Based Syst.* 116, 26–38. doi:10.1016/j.knosys.2016.10.024

Zhou, B., Fang, J. K., Ai, X. M., Yang, C. X., Yao, W., and Wen, J. Y. (2021). Dynamic Var Reserve-Constrained Coordinated Scheduling of LCC-HVDC Receiving-End System Considering Contingencies and Wind Uncertainties. *IEEE Trans. Sust. Energ.* 12 (01), 469–481. doi:10.1109/tste.2020.3006984

Conflict of Interest: Authors SP, XG, XiL, and XuL were employed by the company China Southern Power Grid Company Limited.

The remaining author declares that the research was conducted in the absence of any commercial or financial relationships that could be construed as a potential conflict of interest.

Publisher's Note: All claims expressed in this article are solely those of the authors and do not necessarily represent those of their affiliated organizations, or those of the publisher, the editors and the reviewers. Any product that may be evaluated in this article, or claim that may be made by its manufacturer, is not guaranteed or endorsed by the publisher.

GLOSSARY

BESSs battery energy storage systems

CRF capital recovery factor

DN distribution network

IPDM ideal-point decision method

MMSSA multi-objective memetic salp swarm algorithm

MOPSO multi-objective particle swarm optimization

O&M operation and maintenance

PV photovoltaic

RESs renewable energy sources

SOC state of charge

SSA salp swarm algorithm

TOU time of use

WT wind turbines

Variables

$P_{BESS,i}$ power capacity of the ith BESSs.

$E_{BESS,i}$ energy capacity of the ith BESSs.

$P_{cha,i}(t)$ charging power of the ith BESSs at time t

$P_{dis,i}(t)$ discharging power of the ith BESSs at time t

ρ_{loss} TOU electricity prices

$P_{loss}(t)$ power loss at time t

$P_{grid}(t)$ power fluctuation of the grid connection point at time t

x_{mi}^{j} positions of the ith follower salp in the mth salp chain

F_{m}^{j} position of food source

ω_{h} weights of the hth objective function

n population size of single salp chain

M the number of salp chains

$N_{\mathbf{r}}$ the maximum size of the repository